Available online at www.sciencedirect.com
ScienceDirect
Journal of Photochemistry and Photobiology A: Chemistry 188 (2007) 378–386
Journal of Photochemistry and Photobiology A:Chemistry
www.elsevier.com/locate/jphotochem

Synthesis, absorption, and fluorescence properties and crystal structures of 7-aminocoumarin derivatives

Noriko Kitamura [a], Tomoyoshi Fukagawa [a], Shigeru Kohtani [a,b], Soh-ichi Kitoh [c], Ko-Ki Kunimoto [c], Ryoichi Nakagaki [a,b,*]

[a] *Division of Life Sciences, Graduate School of Natural Science and Technology, Kanazawa University, Kakuma-machi, Kanazawa 920-1192, Japan*
[b] *Faculty of Pharmaceutical Sciences, Kanazawa University, Kakuma-machi, Kanazawa 920-1192, Japan*
[c] *Division of Material Sciences, Graduate School of Natural Science and Technology, Kanazawa University, Kakuma-machi, Kanazawa 920-1192, Japan*

Received 6 October 2006; received in revised form 25 December 2006; accepted 30 December 2006
Available online 4 January 2007

Abstract

Among several newly synthesized coumarins are 7-pyrrolyl coumarins and carbazole-coumarin hybrids (2-pyranone-condensed carbazoles). Their spectral properties and crystal structures are discussed by comparing with those of related 7-aminocoumarin derivatives. Carbazole-coumarin hybrids exhibit absorption properties common to those of 7-aminocoumarins and simple carbazoles.

Keywords: 7-Aminocoumarin derivatives; Synthesis; Absorption properties; Fluorescence properties; Crystal structures

1. Introduction

Coumarins substituted at 7-position with an electron-donating group are known to exhibit strong fluorescence [1]. Since 7-aminocoumarins are highly fluorescent, they have been used as optical brighteners and fluorescent probes. Substituted 7-aminocoumarins also form an important class of laser dyes for the blue-green region. The present authors already reported the absorption and fluorescence spectra of 7-aminocoumarins [2]. Specific hydrogen-bonding effects were observed for 7-aminocoumarins in the highly polar media. The previous study [2] suggests that pyramidalization at the nitrogen atom of the amino coumarin derivatives may be responsible for the observed blue shift and the slight decrease in the molar extinction coefficient or oscillator strength on changing solvent polarity. Fig. 1 shows molecular structure of coumarin with the numbering of skeletal atoms.

This paper is concerned with synthesis, absorption and fluorescence properties, and crystal structures of newly synthesized 7-aminocoumarin derivatives and related compounds. Their spectroscopic properties and crystal structures are discussed in comparison with those of related 7-aminocoumarin derivatives. Fig. 2 shows the chemical structures of compounds which will be discussed in this paper. They are categorized into three major groups. The three major groups can be further classified into eight subgroups. They are bicyclic coumarin derivatives (Type 1: non-cyclic derivatives containing an alkylamino group at 7-position of coumarin), tricyclic coumarin derivatives (Type 2-1: phenylamino-substituted derivatives, Type 2-2: pyrrolyl-substituted derivatives, Type 2-3: an indoline-coumarin hybrid dye, Type 2-4: 1,2,3,4-tetrahydroquinoline-coumarin hybrids), tetracyclic coumarin derivatives (Type 3-1: carbazole-coumarin hybrids-straight form, Type 3-2: carbazole-coumarin hybrids-angular form, Type 3-3: julolidine-coumarin hybrids).

2. Experimental

2.1. General methods

Melting points are uncorrected. ^{1}H NMR spectra were recorded on a JEOL-GSX 500 MHz spectrometer. IR spectra

* Corresponding author at: Division of Life Sciences, Graduate School of Natural Science and Technology, Kanazawa University, Kakuma-machi, Kanazawa 920-1192, Japan. Tel.: +81 76 234 4425; fax: +81 76 234 4484.
E-mail address: nakagaki@p.kanazawa-u.ac.jp (R. Nakagaki).

1010-6030/$ – see front matter © 2007 Elsevier B.V. All rights reserved.
doi:10.1016/j.jphotochem.2006.12.039

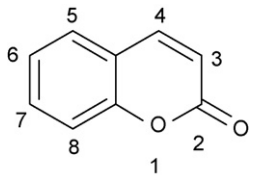

Fig. 1. Molecular structure of coumarin with the numbering of skeletal atoms.

were measured on a Jasco FT/IR-410 infrared spectrometer. Electronic absorption spectra were recorded on a Hitachi U-3210 spectrophotometer. Electronic fluorescence spectra were measured on a Hitachi F-4500 fluorescence spectrophotometer. The fluorescence quantum yield (Φ) was determined by the relative method using the quinine bisulfate (Nakarai Chemicals)/0.1N H_2SO_4 aqueous solution as a standard ($\Phi = 0.52$) [3]. The fluorescence lifetime (τ) measurements were carried out using a nitrogen laser (LTB Lasertechnik Berlin, 337 nm, fwhm 350 ps) as the excitation source. The fluorescence decay signals at the wavelength selected by a monochromator (Ritsu MC-20L) were detected by a photomultiplier tube (Hamamatsu H-3284). Signals from the photomultiplier were recorded on a digital storage oscilloscope (Tektronix TDS 520) interfaced to a personal computer (NEC, PC9801). The fluorescence decay curves thus obtained were analyzed by the deconvolution method involving linearization of the single exponential function and least-squares fitting. The detection limit of the method was estimated to be 100 ps.

2.2. Crystallographic analysis

X-ray crystallographic analysis data collections were performed at 123 K on a Rigaku/MSC Mercury CCD diffractometer with graphite monochromated Mo Kα radiation (λ = 0.71070 Å) and a rotating anode generator for compounds **7**, **8**, **12**, and **14**, while the X-ray data for 4-methyl-4′,5′-dihydropyrrolocoumarin (**10**) were collected at 295 K on a Rigaku AFC7R diffractometer with graphite monochromated Cu Kα radiation (λ = 1.54178 Å) and a rotating anode generator. The data were corrected for Lorentz-polarization effects. The structure was solved by direct methods and expanded using Fourier techniques. All non-hydrogen atoms were refined anisotropically. All hydrogen atoms were refined isotropically. All calculations were performed using the teXsan crystallographic software package.

2.3. Materials

Ethanol (spectroscopic grade) was purchased from Nacalai Tesque and used without further distillation. The following coumarin derivatives were commercially obtained and their synonyms and sources were given in the parenthesis: **1** (Coumarin 120, 7-amino-4-methylcoumarin, Tokyo Kasei Kogyo); **2** (Coumarin 151, 7-amino-4-trifluoromethylcoumarin, Aldrich); **3** (Coumarin 311, 7-*N*,*N*-dimethylamino-4-methylcoumarin, Aldrich); **4** (Coumarin 152, 7-*N*,*N*-dimethylamino-4-trifluoromethylcoumarin, Exciton); **11** (Coumarin 339, 6,7,8,9-tetrahydro-4-methyl-2*H*-pyrano[3,2-*g*]quinolin-2-one,

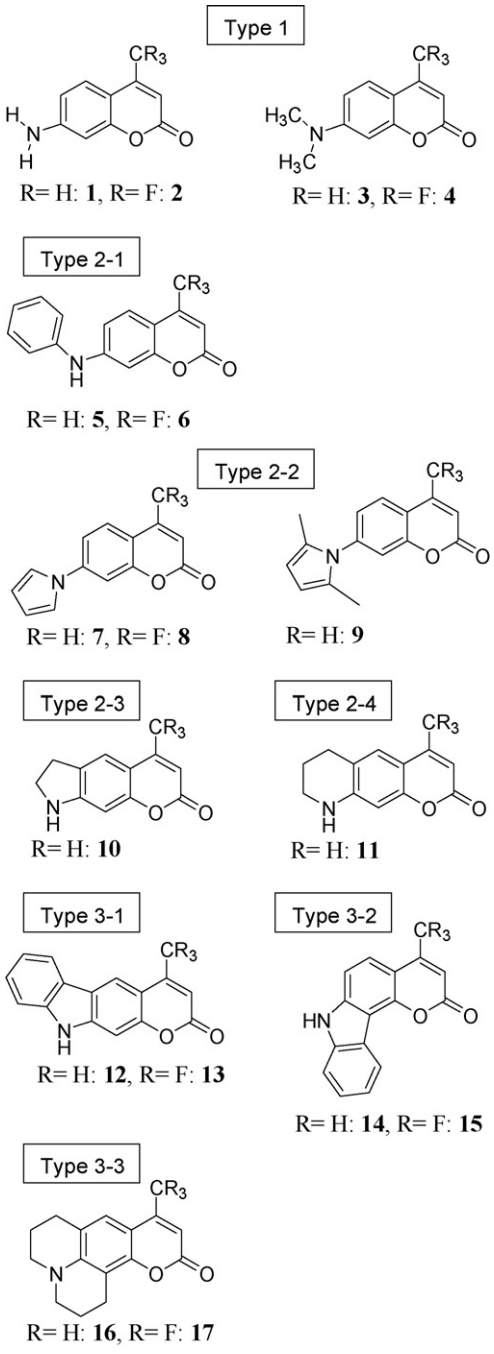

Fig. 2. Chemical structures of 7-aminocoumarins.

Kodak); **16** (Coumarin 102, 2,3,6,7-tetrahydro-9-methyl-1*H*,5*H*,11*H*-pyrano[2,3-*d*]benzo[1,2,3-*ij*]quinolizin-11-one, Exciton); **17** (Coumarin 153, 2,3,6,7-tetrahydro-9-(trifluoromethyl)-1*H*,5*H*,11*H*-[1]benzopyrano[6,7,8-*ij*]-quinolizin-11-one, Aldrich). The most of them are of laser-grade or equivalent. The compounds purchased were used without further purification. 7-Phenylamino-4-methyl-2*H*-1-benzopyran-2-one (**5**) was synthesized according to the procedure reported by Umemoto et al. [4].

7-Phenylamino-4-trifluoromethyl-2*H*-1-benzopyran-2-one (**6**) was synthesized according to the procedure described by Bissell et al. [5]. 4-Methyl-4′,5′-dihydropyrrolocoumarin

(**10**) was synthesized according to the procedure described by Quanten et al. [6]. The synthesis of the following compounds were previously reported:

7-(1*H*-Pyrrol-1-yl)-4-methyl-2*H*-1-benzopyran-2-one (**7**) [7],
7-(l*H*-Pyrrol-l-yl)-4-trifluoromethyl-2*H*-l-benzopyran-2-one (**8**) [8],
10*H*-4-Methyl-2*H*-2-oxopyrano[5,6-*b*]carbazole (**12**) [9], and
7*H*-4-Methyl-2*H*-2-oxopyrano[5,6-*c*]carbazole (**14**) [10].

*2.3.1. 7-(2,5-Dimethyl-1H-pyrrol-1-yl)-4-methyl-2H-1-benzopyran-2-one (**9**)*

A mixture of 1.0 g (5.7 mmol) of 7-amino-4-methylcoumarin and 0.7 g (6.1 mmol) of acetonylacetone was refluxed at 120 °C in 20 ml of acetic acid for 1 h. After a 2% aqueous solution of NaOH was added, the organic layer was extracted with $CHCl_3$. The combined extract was washed with a saturated solution of NaCl. Followed by drying with anhydrous sodium sulfate, the crude product was put on a chromatography column packed with silica gel and eluted with a hexane/ethyl acetate mixture (2/1) (recrystallized from a water/methanol mixture and a hexane/ethyl acetate mixture): yield 15%; m.p. 139–141 °C; MS $m/z = 252$ (M^+); ^{1}H NMR (500 MHz, $CDCl_3$) δ 7.70–7.69 (1H, d), 7.26–7.16 (2H, m), 6.35 (1H, s), 5.94 (2H, s), 2.49 (3H, s), 2.08 (6H, s); IR (KBr, cm^{-1}) 3066, 2916, 1808, 1749, 1727, 1616, 1552, 1519, 1510; UV (λ_{max}, nm (ε, $10^4\ M^{-1}\ cm^{-1}$), C_2H_5OH) 317 (0.9), 283 (0.7), 205 (3.0); Found: C, 75.72; H, 5.97; N, 5.51%. Calcd for $C_{16}H_{15}NO_2$: C, 75.87; H, 5.97; N, 5.53%.

*2.3.2. 10H-4-Trifluoromethyl-2H-2-oxopyrano[5,6-b] carbazole (**13**)*

A mixture of 1.0 g (5.5 mmol) of 2-hydroxycarbazole, 3.5 g (19 mmol) of ethyl 4,4,4-trifluoroacetoacetate and 1.7 g (13 mmol) of anhydrous $ZnCl_2$ was refluxed at 120 °C in 6 ml of dry ethanol for 24 h. The reaction mixture was poured into cold 0.1N hydrochloric acid. The crude product was filtered off, dried in vacuo and put on a chromatography column packed with silica gel and eluted with a hexane/ethyl acetate mixture (9/1): yield 36%; m.p. higher than 300 °C; ^{1}H NMR (500 MHz, $CDC1_3$) δ 8.51 (1H, s), 8.31–8.30 (1H, d), 7.61–7.28 (4H, m), 6.74 (1H, s); MS $m/z = 303$ (M^+); IR (KBr, cm^{-1}) 3267, 1929, 1710, 1635, 1611, 1583, 1568, 1497, 1487; UV (λ_{max}, nm (ε, $10^4\ M^{-1}\ cm^{-1}$), C_2H_5OH) 375 (2.0), 317 (2.5), 285 (2.5), 233 (4.5); Found: C, 63.47; H, 2.76; N, 4.68%. Calcd for $C_{16}H_8F_3NO_2$: C, 63.37; H, 2.65; N, 4.61%.

*2.3.3. 7H-4-Trifluoromethyl-2H-2-oxopyrano [5,6-c]carbazole (**15**)*

4-Hydroxycarbazole was purified by column chromatography packed with silica gel and eluted with a hexane/ethyl acetate mixture (5/1). A mixture of 1.0 g (5.5 mmol) of purified 4-hydroxycarbazole, 2.9 g (16 mmol) of ethyl 4,4,4-trifluoroacetoacetate and 1.6 g (12 mmol) of anhydrous $ZnCl_2$ was refluxed at 120 °C in 6 ml of dry ethanol for 27 h. The reaction mixture was poured into cold water. The crude product was filtered off, dried in vacuo and put on a chromatography column packed with silica gel and eluted with a hexane/ethyl acetate mixture (1/1) (recrystallized from methanol): yield 33%; m.p. higher than 300 °C; ^{1}H NMR (500 MHz, $CDCl_3$) δ 8.46–8.45 (1H, d), 7.76–7.38 (5H, m), 6.77 (1H, s); MS $m/z = 303$ (M^+); IR (KBr, cm^{-1}) 3380, 3105, 1871, 1725, 1637, 1597, 1582, 1569, 1496, 1466; UV (λ_{max}, nm (ε, $10^4\ M^{-1}\ cm^{-1}$), C_2H_5OH) 365 (2.2), 309 (3.7), 279 (2.5), 229 (4.4); Found: C, 63.30; H, 2.69; N, 4.37%. Calcd for $C_{16}H_8F_3NO_2$: C, 63.37; H, 2.65; N, 4.61%.

3. Results and discussion

3.1. Synthesis

Several synthetic methods for coumarins have been investigated [11,12]. One of the most important synthetic procedures is Pechmann synthesis, namely, condensation of phenols with β-keto esters in the presence of Lewis acid catalysts [13]. The present authors have employed this methods for synthesis of **12–15** (Types 3-1 and 3-2) [4,5]. On the other hand, pyrrolyl coumarins (Type 2-2) are derived from 7-aminocoumarins according to the standard method for pyrrole synthesis [14–16].

3.2. Absorption spectra

The spectral data of coumarins in ethanol are listed in Table 1. The lowest energy band shifts to longer wavelengths on going from 4-methyl substitution to 4-trifluoromethyl substitution. This type of shift is clearly observed for the following pairs: **1** and **2**, **3** and **4**, **5** and **6**, **7** and **8**, **12** and **13**, **14** and **15**, and **16** and **17**. These pairs exhibit similar spectral shapes with some red shifts. 4-Methylcoumarins show absorption maxima ranging from (25.8–31.6) × 10^3 cm^{-1}, while 4-trifluoromethylcoumarins show absorption maxima ranging from (23.7–29.2) × 10^3 cm^{-1} (see Table 1).

The spectral shapes for Type 1, Type 2-3, Type 2-4, and Type 3-3 are very similar (see Fig. 3 a). The lowest energy band shifts to longer wavelengths on going from **1** to cyclized species (**10**, **11**, and **16**). The following absorption maxima in 10^3 cm^{-1} were observed for these coumarins: **1** (28.3); **10** (27.0); **11** (26.4); **16** (25.8). Comparison of spectral data for pairs (**1** and **3**, **2**

Table 1
Absorption spectral data for 7-aminocoumarins in ethanol

Group	4-Methylcoumarins		4-Trifluoromethylcoumarins	
Type 1	**1**	28.3 (1.9)	**2**	26.2 (1.8)
	3	27.2 (2.2)	**4**	25.3 (1.9)
Type 2-1	**5**	27.0 (2.6)	**6**	25.2 (2.3)
Type 2-2	**7**	30.4 (1.9)	**8**	29.2 (1.8)
	9	31.6 (1.2)		
Type 2-3	**10**	27.0 (2.3)		
Type 2-4	**11**	26.4 (2.4)		
Type 3-1	**12**	27.4 (2.2)	**13**	26.7 (2.0)
Type 3-2	**14**	28.3 (1.4)	**15**	26.6 (1.2)
Type 3-3	**16**	25.8 (2.3)	**17**	23.7 (2.0)

Absorption maxima are given in 10^3 cm^{-1}. The numbers in parentheses are the molar extinction coefficients in $10^4\ M^{-1}\ cm^{-1}$.

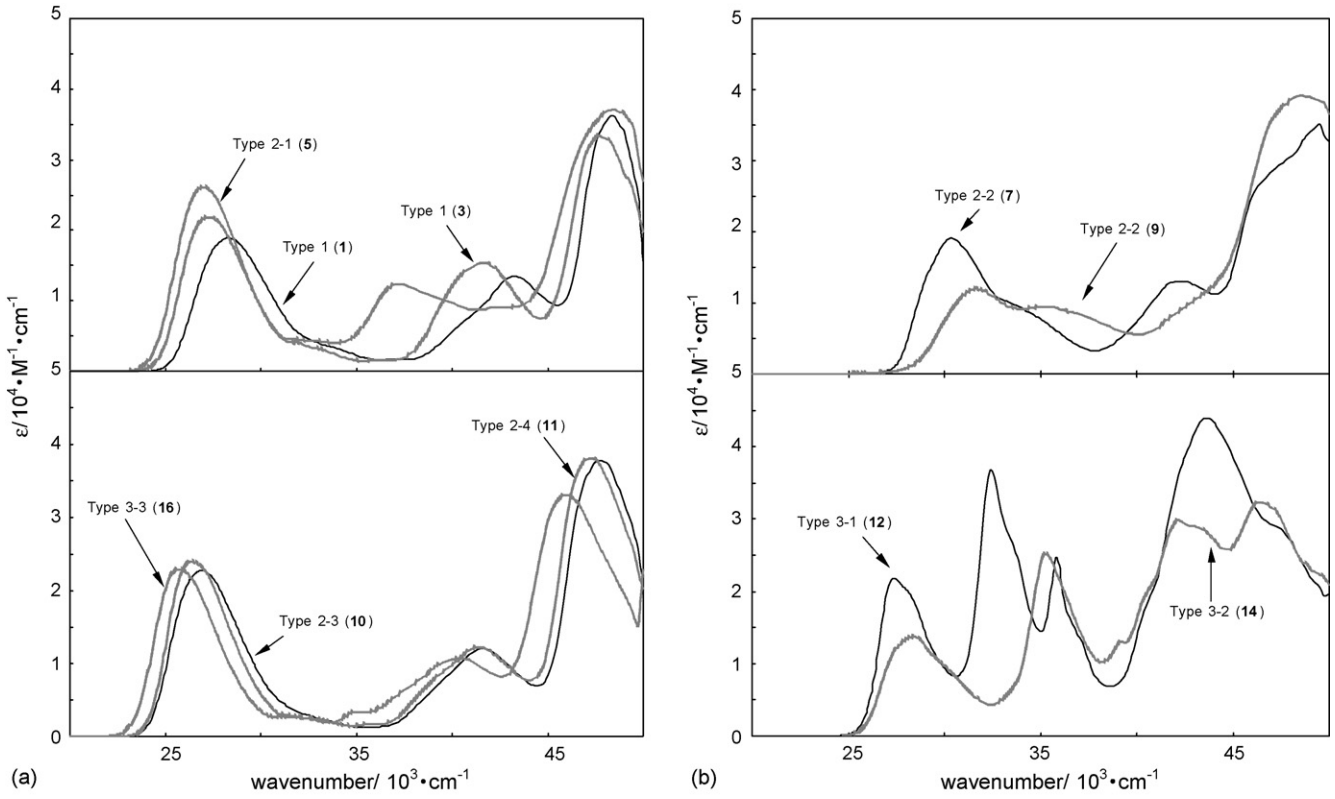

Fig. 3. Absorption spectra of 7-aminocoumarins: (a) **1**, **3**, **5**, **10**, **11**, and **16**; (b) **7**, **9**, **12**, and **14**.

and **4**) shows that alkylation at the amino group leads to the bathochromic shift [17]. The first ionization energies (IE) for aniline derivatives become smaller on alkylation of the amino group and on cyclization by forming bonds between the nitrogen and ring carbons. Typical IE values in eV for substituted anilines are given below: aniline (8.10), *N*,*N*-dimethylaniline (7.45), indoline (7.67), 1,2,3,4-tetrahydroquinoline (7.50), and julolidine (7.05) [18]. The decrease in ionization energies corresponds to the increase in the electron-donating ability. Compounds **10**, **11**, and **16** can be regarded as pyranone-fused indoline, 1,2,3,4-tetrahydroquinoline, and julolidine, respectively. The experimental results listed in Table 1 indicate that the increased electron-releasing ability is responsible for the observed red shifts and the slight increase in the molar extinction coefficients. The bathochromic shift observed for **10**, **11**, and **16** is attributed to the increased electron-donating ability, since the longest wavelength band of the 7-aminocoumarin is characterized as intramolecular charge transfer transition. A similar red shift detected for methylated and trifluoromethylated pair can also be interpreted from the viewpoint of intramolecular charge transfer. In this case trifluoromethylation increases electron-accepting ability of the pyranone moiety.

Since the highest occupied molecular orbital of pyrrole has a node at the nitrogen atom, the connection of 1-pyrrolyl moiety at the 7-position of coumarin may diminish π-conjugation. The observed blue-shift of pyrrolyl coumarin (Type 2-2) is attributable to inefficient π-conjugation.

The absorption spectra of carbazole-coumarin hybrids (Types 3-1 and 3-2) are completely different from those of other coumarins. The spectral shapes for the carbazole-coumarin hybrids are not similar to those for phenylamino-substituted derivatives (Type 2-1) (see Fig. 3a and b), and are closely related with spectral properties of unsubstituted carbazole [19–21]. Since the second lowest energy transition of carbazole is allowed, the second longest wavelength bands of carbazole-coumarin hybrids (Types 3-1 and 3-2) are also allowed peaking around 35×10^3 cm^{-1} with large molar extinction coefficients. The lowest excited singlet state of carbazole is ^1L_b, which means that the longest wavelength band is a forbidden transition, while the second lowest excited singlet state of carbazole is ^1L_a, which appears around 35×10^3 cm^{-1} with $\log \varepsilon = 4.3$ [20]. The absorption bands of carbazole-coumarin hybrids in 270–310 nm region resemble that of unsubstituted carbazole peaking around 35×10^3 cm^{-1}. Since 7-aminocoumarins exhibit no strong absorption bands around 35×10^3 cm^{-1}, the second lowest energy transition of carbazole-coumarin hybrids is mainly attributable to a carbazole chromophore. The lowest energy band of carbazole-coumarin hybrids is closely related with that of 7-aminocoumarin.

3.3. Fluorescence properties

The spectral data and rate constants for radiative and nonradiative decay of coumarins in ethanol are listed in Table 2. Introduction of trifluoromethyl groups causes shifts of emission band to longer wavelengths and decrease in fluorescence quantum yields. Among our newly synthesized 7-aminocoumarins (Types 2-2, 3-1, and 3-2), pyrrolyl- and

Table 2
Fluorescence properties for 7-aminocoumarins in ethanol

Group	4-Methylcoumarins						4-Trifluoromethylcoumarins					
	Compound	$\tilde{\nu}_{emi}$	Φ	τ	k_r	k_{nr}	Compound	$\tilde{\nu}_{emi\,i}$	Φ	τ	k_r	k_{nr}
Type 1	**1**	23.4	0.78	4.0	2.0	0.54	**2**	20.8	0.53	5.7	0.92	0.83
Type 2-1	**5**	21.5	0.004	<0.1	–	–	**6**	20.0	<0.003	–	–	–
Type 2-3	**10**	22.7	0.71	3.9	1.8	0.75						
Type 2-4	**11**	22.5	0.71	4.0	1.8	0.73						
Type 3-1	**12**	21.5	0.14	5.5	0.26	1.6	**13**	18.6	<0.003	–	–	–
Type 3-2	**14**	23.5	0.25	2.1	1.2	3.6	**15**	20.0	0.02	0.8	0.30	12
Type 3-3	**16**	21.3	0.65	4.7	1.4	0.75	**17**	19.0	0.28	5.0	0.55	1.4

Emission maxima ($\tilde{\nu}_{emi}$) are given in 10^3 cm^{-1}. Fluorescence lifetime (τ) are given in ns. Radiative decay rate constants (k_r) and radiationless decay rate constants (k_{nr}) are given in 10^8 s^{-1}.

trifluoromethyl-substituted derivatives (**7**–**9**, **13** and **15**) exhibit weak fluorescence. In particular, fluorescence quantum yields of pyrrolyl compounds (Type 2-2) (**7**–**9**) are not more than 0.003. It has been pointed out that 1-pyrrolyl moiety does not play any role as substituent of fluorescing conjugated systems, while 1-pyrazolyl group act as a constituent of some important optical brighteners [12]. The fact that fluorescent intensity is increased on going from 1-pyrrolyl- to 1-pyrazolyl-substitution at 7-position of coumarin suggests that a symmetry lowering (non-symmetrical ring nitrogen substitution) may increase π-conjugation [12]. This is in accordance with the fact that *N*-phenylpyrrole exhibits relatively weak fluorescence, i.e. the fluorescence quantum yield is of the order of 10^{-2} [22]. Coumarins illustrated in Fig. 2 have molar extinction coefficient with the magnitude of (1–2) × 10^4 M^{-1} cm^{-1}. Trifluoromethylation of coumarins at 4-position does not cause appreciable changes in molar extinction coefficient. Since the radiative transition probability is closely related to the integrated absorption

Table 3
The observed results of the determined compounds

		Bond length (Å)					
		a	b	c	d	e	f
Type 2-2	**7**	1.405 (2)	1.382 (2)	1.408 (2)	1.392 (2)	1.385 (2)	1.400 (2)
	8	1.404 (2)	1.377 (2)	1.408 (2)	1.393 (2)	1.386 (2)	1.403 (2)
Type 2-3	**10**	1.419 (2)	1.357 (2)	1.404 (2)	1.379 (2)	1.380 (2)	1.399 (2)
Type 3-1	**12**	1.402 (3)	1.382 (3)	1.426 (3)	1.385 (3)	1.377 (3)	1.411 (3)
		1.399 (3)	1.391 (3)	1.428 (3)	1.386 (3)	1.381 (3)	1.414 (3)
Type 3-2	**14**	1.417 (3)	1.370 (3)	1.406 (3)	1.411 (3)	1.385 (3)	1.394 (3)
		Bond angles (°)					
		1	2	3	4	5	6
Type 2-2	**7**	116.8 (1)	122.0 (1)	119.7 (1)	119.6 (1)	119.5 (1)	122.5 (1)
	8	116.9 (1)	121.3 (1)	120.5 (1)	119.43 (10)	118.92 (10)	122.9 (1)
Type 2-3	**10**	116.6 (1)	120.7 (1)	120.4 (1)	121.1 (1)	117.5 (1)	123.7 (1)
Type 3-1	**12**	118.3 (2)	120.2 (2)	119.3 (2)	122.0 (2)	116.7 (2)	123.5 (2)
		118.3 (2)	119.8 (2)	119.6 (2)	121.8 (2)	116.8 (2)	123.7 (2)
Type 3-2	**14**	118.3 (2)	122.3 (2)	117.7 (2)	121.9 (2)	118.3 (2)	121.4 (2)
		Bond angles (°)					
		7	8	9	$\sum$		
Type 2-2	**7**	125.3 (1)	126.3 (1)	108.2 (1)	359.8		
	8	125.45 (10)	125.98 (10)	108.46 (10)	359.89		
Type 2-3	**10**	115 (1)	110.3 (2)	123 (1)	348.3		
Type 3-1	**12**	126 (1)	108.9 (2)	123 (1)	357.9		
		124 (1)	108.9 (2)	125 (1)	357.9		
Type 3-2	**14**	109.1 (2)	121 (1)	129 (1)	359.1		

Designation of bond length and angles is shown in Fig. 4. Å (angstrom) is defined as 10^{-10} m.

intensity [23], the magnitude of the radiative transition probability may not be changed on trifluoromethylation. Therefore decrease in fluorescence intensity caused by trifluoromethylation is entirely due to increase in transition probability of radiationless deactivation.

The fluorescence quantum yield, Φ, and the fluorescence lifetime, τ, have been determined in order to clarify the nonradiative decay process of coumarins. We calculated rate constants for radiative (k_r) and nonradiative (k_{nr}) decay by the use of the following equations: $k_r = \Phi/\tau$, and $k_{nr} = (1 - \Phi)/\tau$. The rate constants (k_r and k_{nr}) were listed in Table 2. These values can be regarded as crude estimation, since the measurement of Φ or τ is not very accurate [24]. The radiationless decay rate constant increases on going from 4-methyl substitution to 4-trifluoromethyl substitution. This type of increase is clearly observed for the following pairs: **1** and **2**, **14** and **15**, and **16** and **17**. The magnitude of k_{nr} remains of the same order on going from **1** to cyclized species (**10**, **11**, and **16**). At present, the nature of radiationless decay is not clear, since the quantum yield for intersystem crossing or internal conversion is not determined. Jones and coworkers suggested that the quantum yield for intersystem crossing is small, and that the nonradiative decay is mainly due to the internal conversion [24]. López Arbeloa and collaborators suggested that the internal conversion may be explained by the following two models: (1) the formation of a nonradiative twisted intramoleclar charge transfer state, and/or (2) a planar-to-pyramidal structural change of the amino group [17]. At present it is not yet determined which of the two models is dominant.

The absorption properties change on going from 7-phenylaminocoumarin to 2-pyranone-condensed carbazoles. In addition, the fluorescence quantum yield is appreciably higher for **5** than for **12**. This type of fluorescence enhancement has been well documented for rigidized planar molecules [25]. Relatively large nonradiative rate constants were observed for carbazole-coumarin hybrids (Types 3-1 and 3-2).

3.4. Crystal and molecular structures

We determined the crystal structures of five compounds (**7**, **8**, **10**, **12**, and **14**) [7–10,26]. The structural data observed for these compounds are given in Table 3. Their structural features are discussed in comparison with that of related 7-aminocoumarin derivatives. The structural feature can be analyzed by comparing changes in bond lengths and angles. In order to discuss the molecular structure the designation illustrated in Fig. 4 is used for the aromatic carbon–carbon bonds by alphabets (a–f) and for bond angles by numbers (1–6) and (7–9), respectively.

Table 4
List of compounds whose crystral structures are solved by X-ray analysis

Group name	Compound name	Reference
Type 1	7-Ethylamino-4-(trifluoromethyl)coumarin (Coumarin 500)	[27]
	7-Ethylamino-4,6-dimethylcoumarin	[28]
	7-Diethylamino-4-trifluoromethylcoumarin(7-diethylamino-4-trifluoromethyl-2*H*-1-benzopyran-2-one)	[29]
	7-Dimethylaminocyclopenta[*c*]coumarin (Coumarin 138)	[30]
	7-Amino-4-trifluoromethylcoumarin	[31]
	7-Ethylamino-6-methyl-4-trifluoromethylcoumarin	[32]
	3-(2-Benzimidazolyl)-7-(diethylamino)coumarin	[33]
	7-Dimethylamino-4-trifluoromethylcoumarin (Coumarin 152)	[34,35]
	3-(5-Chloro-2-benzoxazolyl)-7-(diethylamino)-2*H*-1-benzopyran-2-one	[36]
	7-Amino-4-methylcoumarin (Coumarin 120)	[37]
	3-(2-Benzothiazolyl)-7-(diethylamino)coumarin (Coumarin 6)	[38]
	7-(Dimethylamino)-4-methyl-2*H*-1-benzopyran-2-one (Coumarin 311)	[39]
	7-Amino-3-phenylcoumarin	[40]
Type 2-2	7-(1*H*-Pyrrol-1-yl)-4-methyl-2*H*-1-benzopyran-2-one	[7]
	7-(1*H*-Pyrrol-1-yl)-4-trifluoromethyl-2*H*-1-benzopyran-2-one	[8]
Type 2-3	4-Methyl-4′,5′-dihydropyrrolocoumarin	[26]
Type 2-4	6,7,8,9-Tetrahydro-4-methyl-2*H*-pyrano[3,2-*g*]quinolin-2-one (Coumarin 339)	[41]
	6,7,8,9-Tetrahydro-4-trifluoromethyl-2*H*-pyrano[3,2-*g*]quinolin-2-one (Coumarin 340)	[42]
	6,7,8,9-Tetrahydro-9-ethyl-4-trifluoromethyl-2*H*-pyrano[3,2-*g*]quinolin-2-one (Coumarin 355)	
Type 3-1	10*H*-4-Methyl-2*H*-2-oxopyrano[5,6-*b*]carbazole	[9]
Type 3-2	7*H*-4-Methyl-2*H*-2-oxopyrano [5,6-*c*] carbazole	[10]
Type 3-3	10-(1,3-Benzothiazol-2-yl)-2,3,6,7-tetrahydro-1*H*,5*H*-11*H*-[1]benzopyrano[6,7,8-*ij*]-quinoliz-11-one (Coumarin 545)	[43]
	2,3,6,7,10,11-Hexahydro-1*H*,5*H*-cyclopenta [3,4] [1]benzopyrano[6,7,8-*ij*]quinolizin-12-(9*H*)-one (Coumarin 106)	[44]
	10-Cyano-1,2,5,6-tetrahydro-3*H*,7*H*,11*H*-[1]benzopyrano[6,7,8-*ij*]-quinolizin-11-one	[45]
	1,1-Dimethylethyl-2,3,6,7-tetrahydro-11-oxo-1*H*,5*H*,11*H*-[1]benzopyrano[6,7,8-*ij*]-quinolizine-10-carboxylate (Coumarin 338)	[46]
	2,3,6,7-Tetrahydro-9-methyl-1*H*,5*H*,11*H*-pyrano[2,3-*d*]benzo[1,2,3-*ij*]quinolizin-11-one(2,3,6,7-tetrahydro-9-methyl-1*H*,5*H*-quinolizino[9,1-*gh*]coumarin) (Coumarin 102) (Coumarin 480)	[47]
	2,3,6,7-Tetrahydro-9-(trifluoromethyl)-1*H*,5*H*,11*H*-[1]benzopyrano[6,7,8-*ij*]-quinolizin-11-one (Coumarin 153)	[48]
	Ethyl-2,3,6,7-tetrahydro-11-oxo-1*H*,5*H*,11*H*-[1]benzopyrano[6,7,8-*ij*]-quinolizine-10-carboxylate (Coumarin 314)	[49,50]
	2,3,6,7-Tetrahydro-11-oxo-1*H*,5*H*,11*H*-[1]benzopyrano[6,7,8-*ij*]-quinolizine-10-carboxylic acid (Coumarin 343)	[51]

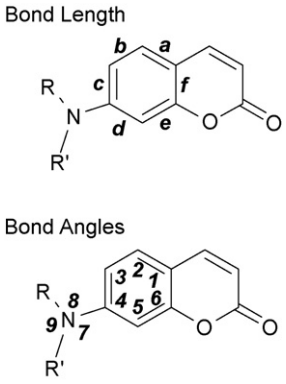

Fig. 4. Designation of bond length and angles.

We have selected 25 crystallographic papers for 24 derivatives from the Cambridge Structural Database and literature [27–51]. The compounds employed for structural discussion are listed in Table 4.

The average values are calculated from crystallographic data in Table 3 and references listed in Table 4. They are summarized in Tables 5 and 6. Since the quality of crystallographic data reported in the literature is not homogeneous, only tendency may be remarked.

3.4.1. Bond length

The aromatic bond length is less sensitive to the condensation with furan [52]. In the case of the 7-aminocoumarin derivatives, the length of bonds b and e are clearly shorter than others. This finding indicates that 7-amino-substitution gives rise to the quinoidal nature in the ground state of 7-aminocoumarins. Bonds c and d in condensed coumarins are longer than other bonds. For example, bond c in the tricyclic condensed coumarins (indoline-coumarin hybrid (Type 2-2), and the 1,2,3,4-tetrahydroquinoline-coumarin hybrids (Type 2-3)) is fairly long, and bond c or d in the carbazole-coumarin hybrid (Types 3-1 and 3-2) is elongated. Bonds c and d in julolidine-coumarin hybrids (Type 3-3) are the longest and the second longest. It is interesting to note that elongation of bond c or d is observed on ring-formation at 6 or 8 positions in coumarin (see Fig. 1). Bonds c and d are lengthened in julolidine derivatives formed on condensation at both 6 and 8 positions.

Table 6
The sum value (°) of angles 7, 8, and 9

	Average	Maximum	Minimum
Type 1	359.7	361.0	357.1
Type 2-2	359.8	359.9	359.8
Type 2-3	348.3	–	–
Type 2-4	359.8	360.0	359.7
Type 3-1	357.9	357.9	357.9
Type 3-2	359.1	–	–
Type 3-3	359.0	360.1	356.1

Designation of bond angles is shown in Fig. 4.

3.4.2. Bond angles

Bond angles in aromatic ring of coumarins change on going from unsubstituted coumarins to furano-condensed coumarins [52]. On the other hand, the bond angle in aromatic rings are less sensitive to substitution in the case of 7-aminocoumarin derivatives. The angle 4 between bond c and d is generally larger than the adjacent angles (3 and 5) for carbazole-coumarin hybrids (Types 3-1 and 3-2). Crystallographic data in literature [53–57] clearly show that the magnitude of angle 4 is generally larger than that of angle 5. The structural data for simple carbazoles are listed in Table 7.

The sum of bond angles around the nitrogen atom of 7-position is 348° in the case of the indoline-coumarin hybrid

Table 5
Average values for structural parameters calculated for seven groups of compounds

	Bond length (Å)					
	a	b	c	d	e	f
Type 1	1.404 (22)	1.366 (22)	1.415 (21)	1.401 (21)	1.372 (21)	1.394 (20)
Type 2-2	1.405 (3)	1.380 (3)	1.408 (3)	1.393 (3)	1.386 (3)	1.402 (3)
Type 2-3	1.419 (2)	1.357 (2)	1.404 (2)	1.379 (2)	1.380 (2)	1.399 (2)
Type 2-4	1.405 (8)	1.369 (8)	1.421 (8)	1.402 (8)	1.371 (8)	1.394 (8)
Type 3-1	1.401 (4)	1.387 (4)	1.427 (4)	1.386 (4)	1.379 (4)	1.413 (4)
Type 3-2	1.417 (3)	1.370 (3)	1.406 (3)	1.411 (3)	1.385 (3)	1.394 (3)
Type 3-3	1.405 (10)	1.367 (11)	1.430 (11)	1.413 (9)	1.379 (10)	1.402 (9)
	Bond angles (°)					
	1	2	3	4	5	6
Type 1	116.0 (14)	121.9 (16)	121.1 (15)	117.6 (14)	119.7 (15)	123.6 (15)
Type 2-2	116.9 (1)	121.7 (1)	120.1 (1)	119.515 (1)	119.21 (1)	122.7 (1)
Type 2-3	116.6 (1)	120.7 (1)	120.4 (1)	121.1 (1)	117.5 (1)	123.7 (1)
Type 2-4	115.6 (6)	123.4 (6)	119.0 (6)	118.8 (6)	119.6 (6)	123.5 (6)
Type 3-1	118.3 (3)	120.0 (3)	119.5 (3)	121.9 (3)	116.8 (3)	123.6 (3)
Type 3-2	118.3 (2)	122.3 (2)	117.7 (2)	121.9 (2)	118.3 (2)	121.4 (2)
Type 3-3	116.8 (7)	122.4 (7)	119.4 (7)	119.7 (7)	118.0 (7)	123.7 (7)

Designation of bond length and angles is shown in Fig. 4.

Table 7
The observed results for carbazoles

Compounds	1	2	3	4	5	6	Reference
Carbazole	120.1	117.9	120.6	121.9	115.6	123.9	[53]
N-Vinylcarbazole	120.8	118.6	120.1	121.5	117.0	122.1	[53]
Bis(1-carbazolyl)butadiyne	121.0	118.9	118.8	122.9	117.0	121.4	[54]
	121.4	119.0	118.7	122.9	117.0	121.0	
1-Azacarbazole	121.0	119.2	119.6	121.3	117.9	121.0	[55]
Carbazole	121.0	118.4	119.7	122.3	116.7	122.0	[56]
Ethyl 4-methyl-9*H*-carbazole-3-carboxylate	121.9	118.9	117.9	123.1	117.6	120.7	[57]
	119.4	117.6	120.8	121.3	117.4	123.4	
Average	120.8	118.6	119.5	122.2	117.0	121.9	

Designation of bond angles is shown in Fig. 4.

derivative (Type 2-3). This value indicates that the nitrogen is neither purely sp^3-hybridized nor purely sp^2-hybridized. The sum of bond angles in the indoline-coumarin hybrid derivative (348°) is smaller than the corresponding value, ca. 360° in other categories of coumarins. The amino moiety in the indoline-coumarin hybrid derivative is pyramidal and not coplanar with the rest of the molecules, while the plane defined by the other compounds is coplanar with the molecular plane of coumarin.

4. Summary

The absorption and fluorescence properties and crystal structures of 7-aminocoumarins and related compounds were discussed. The longest wavelength absorption band is characterized as intramolecular charge-transfer transition, since the bathochromic shift is caused by structural modification which increases electron-donating or -accepting ability. The fluorescence quantum yield is remarkably enhanced on going from 2-phenylaminocoumarin to 2-pyranone-condensed carbazoles. Molecular geometry determined by X-ray crystal analysis indicates bond alternation in the ground state.

Acknowledgement

This work was partly supported by a Grant-in-Aid for Scientific Research on Priority Area "Fundamental Science and Technology of Photofunctional Interface" (Area 417) from MEXT of Japan.

References

[1] K.H. Drexhage, in: F.P. Schäfer (Ed.), Dye Lasers, Springer-Verlag, New York, 1973, pp. 144–193.
[2] R. Nakagaki, N. Kitamura, I. Aoyama, H. Ohtsubo, J. Photochem. Photobiol. A: Chem. 80 (1994) 113–119.
[3] S.R. Meech, D. Phillips, J. Photochem. 23 (1983) 193–217.
[4] H. Umemoto, T. Kitao, K. Konishi, Kogyokagakuzasshi 73 (1970) 1146–1151.
[5] E.R. Bissell, D.K. Larson, M.C. Croudace, J. Chem. Eng. Data 26 (1981) 348–350.
[6] E. Quanten, P. Adriaens, F.C. De Schryver, R. Roelandts, H. Degreef, Photochem. Photobiol. 43 (1986) 485–492.
[7] T. Fukagawa, N. Kitamura, S. Kohtani, S. Kitoh, K.-K. Kunimoto, R. Nakagaki, Anal. Sci. 22 (2006) xl87–xl88.
[8] T. Fukagawa, N. Kitamura, S. Kohtani, S. Kitoh, K.-K. Kunimoto, R. Nakagaki, Anal. Sci. 22 (2006) xl89–xl90.
[9] T. Fukagawa, N. Kitamura, S. Kohtani, S. Kitoh, K.-K. Kunimoto, R. Nakagaki, Anal. Sci. 22 (2006) xl91–xl92.
[10] T. Fukagawa, N. Kitamura, S. Kohtani, S. Kitoh, K.-K. Kunimoto, R. Nakagaki, Anal. Sci. 22 (2006) x219–x220.
[11] B.M. Krasovitskii, B.M. Bolotin, Organic Luminescent Materials, VCH Publisher, Weinheim, 1988.
[12] A. Dorlars, C.-W. Schellhammer, J. Schroeder, Angew. Chem., Int. Ed. Engl. 14 (1975) 665–679.
[13] S. Sethna, R. Phadke, Org. React. 7 (1953) 1–58.
[14] R.A. Jones, Aust. J. Chem. 19 (1966) 289–296.
[15] W. Rettig, F. Marschner, Nouv. J. Chim. 7 (1983) 425–431.
[16] G.R. Newkome, W.W. Paudler, Contemporary Heterocyclic Chemistry, Wiley, New York, 1982, pp. 17–45.
[17] T.L. Arbeloa, F.L. Arbeloa, I.L. Arbeloa, J. Luminescence 68 (1996) 149–155.
[18] J.P. Maier, D.W. Turner, J. Chem. Soc. Faraday Trans. II 69 (1973) 521–531.
[19] H.H. Jaffé, M. Orchin, Theory and Applications of Ultraviolet Spectroscopy, John Wiley and Sons, Inc., New York/London, 1962.
[20] I.B. Berlman, Handbook of Fluorescence Spectra of Aromatic Molecules, second ed., Academic Press, New York/London, 1971.
[21] J.E. Adams, W.W. Mantulin, J.R. Huber, J. Am. Chem. Soc. 22 (1973) 5477–5481.
[22] C. Cornelissen-Gude, W. Rettig, J. Phys. Chem. A 102 (1998) 7754–7760.
[23] C.A. Parker, Photoluminescence of Solutions, Elsevier Publishing Company, Amsterdam/London/New York, 1968.
[24] G. Jones II, W.R. Jackson, C.-Y. Choi, W.R. Bergmark, J. Phys. Chem. 89 (1985) 294–300.
[25] T. Förster, Fluoreszenz Organischer Verbindungen, Vandenhoeck & Ruprecht, Göttingen, 1951, pp. 109–113.
[26] N. Kitamura, Y. Toriumi, S. Kohtani, R. Nakagaki, Anal. Sci. 21 (2005) xl01–xl02.
[27] J.P. Jasinski, J.M. Jasinski, Y. Li, D.J. Crosby, Acta Cryst E59 (2003) o153–o154.
[28] K. Chinnakali, K. Sivakumar, S. Natarajan, Acta Cryst. C45 (1989) 1065–1066.
[29] K. Chinnakali, K. Sivakumar, S. Natarajan, Acta Cryst. C48 (1992) 1859–1862.
[30] J.P. Jasinski, R.C. Woudenberg, Acta Cryst. C51 (1995) 107–109.
[31] S. Selladurai, K. Subramanian, Acta Cryst. C48 (1992) 281–283.
[32] K. Chinnakali, K. Sivakumar, S. Natarajan, Acta Cryst. C48 (1992) 386–387.
[33] K. Chinnakali, K. Sivakumar, S. Natarajan, Acta Cryst. C46 (1990) 405–407.
[34] K. Chinnakali, K. Sivakumar, S. Natarajan, Acta Cryst. C46 (1990) 833–835.
[35] J.P. Jasinski, E.S. Paight, Acta Cryst. C50 (1994) 1928–1930.
[36] N.N. Dhaneshwar, S.S. Tavale, T.N. Guru Row, Acta Cryst. C44 (1988) 1858–1860.

[37] J.P. Jasinski, R.C. Woudenberg, Acta Cryst. C50 (1994) 1954–1956.
[38] J.P. Jasinski, E.S. Paight, Acta Cryst. C51 (1995) 531–533.
[39] B.-C. Yip, O.-L. Yaw, L.-H. Ong, H.-K. Fun, K. Sivakumar, Acta Cryst. C51 (1995) 2087–2089.
[40] T. Honda, I. Fujii, N. Hirayama, N. Aoyama, A. Miike, Acta Cryst. C52 (1996) 899–901.
[41] J.P. Jasinski, R.C. Woudenberg, Acta Cryst. C49 (1993) 1965–1967.
[42] J.P. Jasinski, J.M. Jasinski, Y. Li, Acta Cryst. C54 (1998) 410–412.
[43] J.P. Jasinski, Y. Li, Acta Cryst. E58 (2002) o1312–o1314.
[44] T. Honda, I. Fujii, N. Hirayama, N. Aoyama, A. Miike, Acta Cryst. C52 (1996) 364–365.
[45] K. Chinnakali, S. Selladurai, K. Sivakumar, K. Subramanian, S. Natarajan, Acta Cryst. C46 (1990) 837–839.
[46] T. Honda, I. Fujii, N. Hirayama, N. Aoyama, A. Miike, Acta Cryst. C52 (1996) 2363–2365.
[47] K. Chinnakali, K. Sivakumar, S. Natarajan, Acta Cryst. C46 (1990) 669–671.
[48] B.-C. Yip, F.-M. Moo, K.-S. Lok, H.-K. Fun, K. Sivakumar, Acta Cryst. C52 (1996) 477–481.
[49] B.-C. Yip, H.-K. Fun, K. Sivakumar, Z.-Y. Zhou, O.B. Shawkataly, S.-G. Teoh, Acta Cryst. C51 (1995) 956–958.
[50] T. Honda, I. Fujii, N. Hirayama, N. Aoyama, A. Miike, Acta Cryst. C52 (1996) 395–397.
[51] T. Honda, I. Fujii, N. Hirayama, N. Aoyama, A. Miike, Acta Cryst. C52 (1996) 679–681.
[52] N. Kitamura, S. Kohtani, R. Nakagaki, J. Photochem. Photobiol. C: Rev. 6 (2005) 168–185.
[53] K. Tsutsui, K. Hirotsu, M. Umesaki, M. Kurahashi, A. Shimada, T. Higuchi, Acta Cryst. B32 (1976) 3049–3053.
[54] J.J. Mayerle, M.A. Flandera, Acta Cryst. B34 (1978) 1374–1376.
[55] K. Suwińska, Acta Cryst. C41 (1985) 973–975.
[56] R.E. Gerkin, W.J. Reppart, Acta Cryst. C42 (1986) 480–482.
[57] T. Hökelek, S. Patir, Y. Ergün, G. Okay, Acta Cryst. E58 (2002) o206–o208.